JOURNAL OF AGRICULTURAL AND FOOD CHEMISTRY
ARTICLE

J. Agric. Food Chem. 2009, 57, 3563–3570 3563
DOI:10.1021/jf803668e

Monitoring Secondary Structural Changes in Salted and Smoked Salmon Muscle Myofiber Proteins by FT-IR Microspectroscopy

Izaskun Carton,*[,†,‡] Ulrike Bocker,[†] Ragni Ofstad,[†] Oddvin Sørheim,[†] and Achim Kohler[†,§,∥]

[†]Matforsk AS, Nofima Food, and Centre for Biospectroscopy and Data Modelling, Osloveien 1, N-1430 Ås, Norway, [‡]Food Technology, Faculty of Pharmacy, University of the Basque Country (EHU-UPV), Paseo de la Universidad No. 7, 01006 Vitoria-Gasteiz, Spain, [§]CIGENE, Centre for Integrative Genetics, Norwegian University of Life Sciences, N-1432 Ås, Norway and [∥]Department of Mathematical Sciences and Technology (IMT), Norwegian University of Life Sciences, N-1432 Ås, Norway

Fourier transform infrared (FT-IR) microspectroscopy and light microscopy were used to study changes in the myofibrillar proteins and microstructure in salmon muscle due to dry salting and smoking. Light microscopy showed that the myofibers of the smoked samples were more shrunken and their shape more irregular and edged than for the nonsmoked samples. FT-IR microspectroscopy showed that salting time mostly contributed in the amide I region, revealing that secondary structural changes of proteins were primarily affected by salting. The main variation in the amide II region was caused by smoking. As it is known that smoke components can react with amino acid side chains and that the contribution of the side chain in the amide II region is larger than that in amide I, it is concluded that the observed differences are due to interactions between carbonyl compounds of smoke and amino acid side chains.

KEYWORDS: FT-IR microspectroscopy; myofibrillar proteins; salmon; salting; smoking

INTRODUCTION

Traditionally, cold smoked salmon is a highly valued product. Cold smoking is a process by which the fish is submitted to salting before being smoked at temperatures around 25 °C without further heat treatment. It is categorized as a lightly preserved product, and thus, there is a need for improved knowledge about which processing parameters influence product quality.

Salting is the first step in the smoking process and is crucial to obtain high shelf life, good quality, and yield of the product. The salt may be added through dry salting, brine salting, or injection. Dry salting is the most common technique for processing cold smoked salmon (*1*). Salting time varies between smoke houses from hours to several days (*2*). Salting is known to influence the texture properties and water holding capacity (*3*). Barat and co-workers (*4*) suggested that during salting some of the proteins are denatured and precipitate as a result of the high ionic forces in the media, giving rise to textural changes in the product. A recent study by Bocker and co-workers (*5*) investigated the effects of brine salting (16% NaCl) on protein structure in Atlantic salmon muscle tissue with respect to raw material variation. The highest salt uptake was achieved for frozen/thawed (4.1%), followed by postrigor (3.0%), and prerigor (2.2%) salmon. They observed that samples with a lower salt uptake experienced less swelling of the myofibers.

*Corresponding author. Phone: +34 943 01 30 84. E-mail: izaskun.carton@ehu.es.

It is known that the smoking process increases the shelf life of fish as a result of the combined effects of dehydration, antimicrobial (*6*), and antioxidant activity (*7*) of several of the smoke components such as formaldehyde, carboxylic acids, and phenols (*8*, *9*). Few studies have addressed the effect of the smoking process in salmon myofibrillar proteins. Most of the authors suggested that salt is the most important factor for textural and microstructural changes. Sigurgisladottir and co-workers (*10*) demonstrated that salmon muscle fibers shrink during the smoking process. It was also shown that the amount of salt-soluble proteins in salmon is reduced by smoking (*11*, *12*). Previous studies report that interactions between smoke components and amino groups of proteins exist, especially formaldehyde as a smoke component, with the ε-amino group of lysine (*13*−*17*).

Although it is known that the smoking process evokes reactions with amino acid side chains, the influence of the smoking process on protein secondary structure and textural properties is still a rather unexplored field. Fourier transform infrared (FT-IR) spectroscopy has been widely used to study protein secondary structure (*18*), and in recent years, it has become an increasingly powerful tool for the analysis of protein secondary structure in intact food tissues (*5*, *19*−*24*). The main advantage of FT-IR microspectroscopy is that it can be easily combined with histological investigations, as it requires a similar sample preparation, and thus, specific features can be studied on parallel sections both spectroscopically and histochemically. Kirschner and co-workers (*19*)

© 2009 American Chemical Society Published on Web 3/17/2009

used FT-IR-microspectroscopy to monitor heat-induced denaturation in beef muscle. Recently, this technique has been used to characterize processing-induced changes (salting and heating among others) on the myofibrillar protein structure of pork muscle and salmon fillets (*5*, *20*−*24*).

The objetive of this article was to investigate structural changes in salmon muscle during salting and smoking by FT-IR microspectroscopy and light microscopy. While the effect of salting on protein structure has been previously studied by FT-IR microspectroscopy, we intended to investigate if this technique can detect changes of protein secondary structure as a function of smoking.

MATERIALS AND METHODS

Sample Preparation. Nine farmed salmon (*Salmo salar*) of different sizes (small, 3−4 kg; medium, 4−5 kg; and large, 5−6 kg) were acquired from a commercial fish company (Bremnes Seashore AS, Bremnes, Norway). After gutting and cleaning, they were manually filleted prerigor on the day of harvest. To study the influence of the salting time, 6 of the 9 salmons were dry salted at 4 °C, their left fillets for 24 h, and right fillets for 8 h. After salting and an equilibration period of 4 days at 4 °C, half of the samples were smoked: 3 fillets from each type of salting were smoked in a smoking chamber (Unimatic Smoking Unit equipped with a Unitronic SC 2000 Control Unit, Doleschal, Austria) with smoke generated from beech wood for 5.5 h at 28 °C. Finally, 3 of the 9 salmons were used for collecting unprocessed samples. Moreover, all individual fillets were weighed out before and after each process to know the weight loss caused by salting or smoking.

This resulted in a total of 5 different groups: (1) unprocessed samples ($n = 3$), (2) samples salted for 8 h ($n = 3$), (3) samples salted for 24 h ($n = 3$), (4) samples salted for 8 h followed by smoking ($n = 3$), and (5) samples salted for 24 h followed by smoking ($n = 3$). Sampling for chemical analyses (salt and fat determination) was done for each condition at the head and tail regions. Aditionally, for light microscopy and FT-IR microspectroscopy, samples from the skin side (approximately 2 mm from the skin) and inside locations (approximately 30 mm from the skin) were also taken at the head and tail regions for each individual, respectively. Blocks of about 0.7 cm × 0.7 cm × 0.2 cm were excised and embedded in OCT compound (Tissue-Tek, Electron Microscopy Sciences, Hatfield, PA) and then snap-frozen in liquid N_2. The samples were stored at −80 °C until cryosectioning for light microscopy and FT-IR measurements. Ten micrometer thick cryosections were cut on a Leica CM3050S Cryostat (Leica, Nussloch, Germany).

Chemical Analysis. NaCl content in the samples was determined as water soluble Cl^- by titration with a Corning Salt Analysator 926 (Chloride analyzer 926 Corning, Corning Medical and Scientific, Halstead, England) (*25*). The fat content was measured using a low-field ^1H NMR instrument (Maran Ultra, 23 MHz, Oxford 5 Instruments, UK). The instrument was calibrated with refined salmon oil prior to analysis. Except for temperature standardization, no further sample preparation was performed. The weight of the fillets was registered before (w1) and after (w2) each process to calculate the weight loss according to the following equation (**1**):

$$\text{weight loss } \% = (w1 - w2)/w1 \times 100 \quad (1)$$

The results given in **Table 1** for salt and fat content are based on duplicated determinations and are presented as average values together with their standard deviations. In addition, the significance of the differences was determined by use of the *t*-test.

Light Microscopy. For light microscopy, cryosections were stained with 1 g/100 mL Toluidine Blue (Sigma-Aldrich Norway AS, Oslo, Norway) to elucidate the general structure of the muscle samples. The sections were examined with a Leica DM 6000B microscope (Leica Microsystems Wetzlar GmbH, Wetzlar, Germany), and images were acquired at 10× magnification with an Evolution MP 5.0 CCD Camera (Media Cybernetics, The Imaging Experts Silver Springs, Maryland, USA). The images taken as light micrographs correspond to the same areas from which spectra were collected by FT-IR microspectroscopy on parallel cryosections.

FT-IR Microspectroscopy and Preprocessing of the FT-IR Spectra. For FT-IR microspectroscopy, the cryosections were thaw-mounted on 3 mm thick ZnSe slides and were stored overnight in a desiccator at room temperature before the measurements. The FT-IR measurements were carried out with an IRscope II combined with an Equinox 55 FT-IR spectrometer (both Bruker Optics, Germany). Spectra were collected from single myofibers in transmission mode in the frequency range from 4000 to 1000 cm^{-1} using a mercury cadmium telluride (MCT) detector. For each spectrum, 256 interferograms were coadded and averaged at a resolution of 6 cm^{-1}. The microscope and the spectrometer were purged with dry air to reduce spectral contributions from water vapor and CO_2. A background spectrum of the ZnSe substrate was recorded before each spectrum was measured in order to account for variations in water vapor and CO_2.

For every sample, two different blocks were analyzed. From every block, one cryosection was prepared, and three spectra were acquired from three different myofibers per section resulting in a total of 180 spectra: 3 spectra from each cryosection × 4 locations (skin side and inside at the head and tail regions, respectively) × 5 conditions (unprocessed, salted for 8 h, salted for 24 h, salted for 8 h with subsequent smoking, and salted for 24 h with subsequent smoking) × 3 biological replicates (individual fishes) per condition. Spectra were preprocessed by taking second derivatives applied a nine point Savitzky-Golay filter (*26*), followed by extended multiplicative signal correction in the spectral range 3200−1000 cm^{-1} (*27*).

Data Analysis. The 180 FT-IR spectra from each block were averaged resulting in just one spectrum per experimental condition, in total 60 mean spectra. The data analysis was carried out using principal component analysis (PCA) and partial least squares regression (PLSR). PCA was used for the extraction and interpretation of systematic variance in multidimensional data sets by means of a small number of noncorrelated variables. PCA finds directions in the data that explain most of the variation (*28*). These new orthogonal directions are linear combinations of the original ones and are ordered with respect to the amount of explained variance. In this article, PCA was used to investigate the variation in amide I and II regions as a function of salting and smoking processes. Multivariate analysis was done both on mean-spectra and on nonaveraged spectra, resulting in the same variation patterns.

In PLSR, only that part of the main variation in a data matrix **X** is extracted that at the same time maximizes the variation in a data matrix **Y**, i.e., PLSR aims at using only the most relevant part of the variation in **X** for the regression of **Y**, while the unstable or irrelevant variation in **X** is left out of the calculation. In this study, the design variables were used as the **X**-matrix, and the measured variables (FT-IR data) were used as the **Y**-matrix (*28*). The results of PLSR were then studied using so-called correlation loading plots. The correlation loading plot shows the correlation of the **X** and **Y** variables to the PLSR components (scores). Since in second-derivative spectra minima are referring to spectral bands, the

Table 1. General Sample Characteristics for Nonsmoked and Smoked Salmon Fillets[a]

		% weight loss		% NaCl (s)		% fat	
size (location)		24 h	8 h	24 h	8 h	24 h	8 h
nonsmoked	small	6.36	5.50				
	(H)			2.47 ± 0.07	1.57 ± 0.03**	18.9 ± 0.4	14.4 ± 0.1
	(T)			3.88 ± 0.16^{c}	2.29 ± 0.06**,^{c}	4.3 ± 0.2	4.9 ± 0.1
	medium	6.24	4.85				
	(H)			2.46 ± 0.07	1.63 ± 0.03**	16.2 ± 0.4	17.9 ± 0.1
	(T)			3.28 ± 0.12^{b}	1.79 ± 0.04**,^{b}	7.0 ± 0.4	5.4 ± 0.2
	large	6.74	4.23				
	(H)			1.91 ± 0.04	1.76 ± 0.03*	17.8 ± 0.1	18.1 ± 0.1
	(T)			3.32 ± 0.12^{c}	2.29 ± 0.06**,^{c}	8.3 ± 0.0	5.1 ± 0.4
smoked	small	9.77	9.17				
	(H)			3.57 ± 0.07^{C}	2.05 ± 0.07**,^{C}	15.6 ± 0.5	16.7 ± 0.0
	(T)			4.74 ± 0.22^{b,B}	2.87 ± 0.09**,^{c,B}	5.4 ± 0.1	6.1 ± 0.1
	medium	8.91	7.41				
	(H)			2.47 ± 0.07^{A}	1.52 ± 0.07**,^{B}	19.6 ± 0.4	16.1 ± 0.5
	(T)			2.54 ± 0.08^{a,C}	2.46 ± 0.07^{ns,c,C}	5.8 ± 0.0	4.9 ± 0.6
	large	8.86	7.51				
	(H)			3.17 ± 0.07^{C}	1.95 ± 0.07**,^{B}	19.8 ± 0.2	14.3 ± 0.5
	(T)			4.08 ± 0.18^{b,B}	2.50 ± 0.07**,^{c,A}	7.0 ± 0.4	7.8 ± 0.3

[a] H indicates samples from the head and T samples from the tail region of the fillet. (s) Significance level. Between salted for 24 and 8 h: ns, not significant; * $p < 0.05$; ** $p < 0.01$. Between head and tail samples: a, not significant; b, $p < 0.05$; c, $p < 0.01$. Between nonsmoked and smoked samples: A, not significant; B, $p < 0.05$; C, $p < 0.01$.

spectra were multiplied by −1 before analysis by PLSR in order to facilitate interpretation.

All preprocessing and data analysis were performed using an in-house program written in Matlab version 7.3 (The MathWorks, Natick, MA) and using The Unscrambler version 9.2 (Camo Process AS, Norway).

RESULTS AND DISCUSSION

Chemical Analysis and Microstructure. Table 1 shows the results obtained for weight loss, salt, and fat content in processed samples, expressed as percentage values, together with their standard deviation, and the significance level between samples. As expected, salt contents are significantly higher in samples salted for 24 h compared to the samples salted for 8 h. Moreover, the highest salt contents are found in the tail samples. A significant effect of salt concentration on weight loss ($P < 0.05$) is observed, being on average 6.45% ± 0.26 and 4.86% ± 0.64 for samples salted for 24 and 8 h, respectively. As it could also be observed in **Table 1**, the fat distribution on the studied fillets is not homogeneous, as has been demonstrated by other authors (*5*, *29*), decreasing from the head region (17.1% ± 1.9) toward the tail (6.0% ± 1.3). In addition, the flesh near the tail is thinner than that in the head region. Therefore, the salt penetrates more deeply in the tail part. Several authors have reported that the salt uptake in muscle is reduced by increasing fat content (*30*, *31*).

Moreover, smoking shows significant effects on weight loss ($P < 0.001$), which can be ascribed to the dehydration of the flesh after the smoking process. Therefore, salt concentrations are higher in smoked samples than in nonsmoked ones. In addition, salt content and weight loss values for smoked fillets show that samples salted for 24 h contained generally more salt than the samples salted only for 8 h. The weight loss of the fillets decreases from 9.18% ± 0.51 to 8.03% ± 0.99 as a function of salting time.

Figure 1 shows selected images of transverse cryosections of samples from the head region. As can be observed, unprocessed samples exhibit a structure with the myofibers appearing well-attached. For the unprocessed sample, there is no microstructural difference between the skin side and the inside. After salting, clear differences between the inside and the skin side can be seen. The inside samples are more detached, and the extracellular spaces increase with the salting time. This is due to the fact that during dry salting, the salt ions diffuse through the muscle tissue by osmotic forces between the surrounding brine and the muscle, showing shrinkage of the muscle fibers. The differences between the skin side and inside samples can be explained by the fact that the lipid content of the skin side is higher, leading to a decrease of salt diffusivity (*32*).

After the smoking process, the differences appear to be even larger. After salting for 24 h, the myofibers of the smoked samples appear to be more shrunken, and their shape appears more irregular and edged than for the nonsmoked samples. This is in agreement with the results obtained by Sigurgisladottir and co-workers (*10*). After salting for 8 h, the effect of smoking was not so strong. Also, the skin side part of the smoked samples was subjected to only minor changes.

FT-IR Microspectroscopy. Figure 2 displays a typical spectrum of a single myofiber obtained from a fresh salmon muscle cryosection in the spectral region from 4000 to 1000 cm^{-1}. This spectrum represents the most typical features observed for the 5 groups investigated. Amide I (1700−1600 cm^{-1}) is the most dominant band in the myofiber spectrum. Of all the amide bands, of which there exist nine, amide I was found to be the most useful for the analysis of secondary structure of proteins because of its sensitivity to hydrogen-bonding pattern, dipole−dipole interaction, and the geometry of the polypeptide backbone (*18*, *33*). It is mainly affected by the C=O stretching vibration with a minor contribution of C−N stretching and N−H bending vibrations. To enhance spectral resolution and gain insight into changes related to the secondary structure of the myofibrillar proteins, the amide I regions was investigated as second derivative spectra. In the upper left corner of **Figure 2**, the corresponding second derivative spectrum in the amide I region for two exemplary spectra of unprocessed and processed samples is shown. In the second derivative spectra of the amide I region, we were able to identify and assign 9

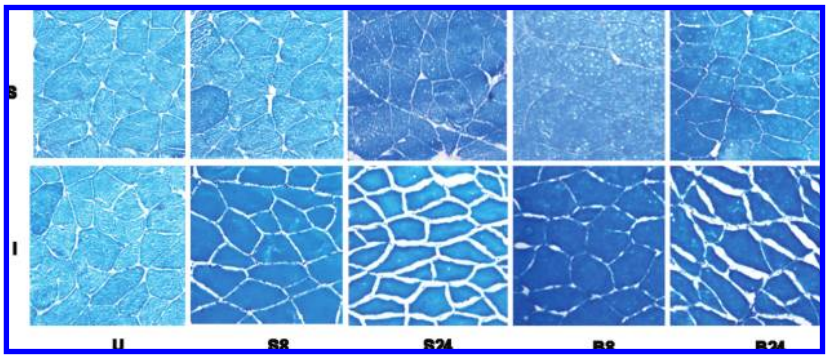

Figure 1. Transverse sections of salmon muscle stained with Toluidine Blue. S refers to the skin side, I to inside, U to unprocessed samples, S8 to salted for 8 h, S24 salted for 24 h, B8 salted for 8 h followed by smoking, and B24 salted for 24 h followed by smoking. All images shown were derived from the head region of the salmon.

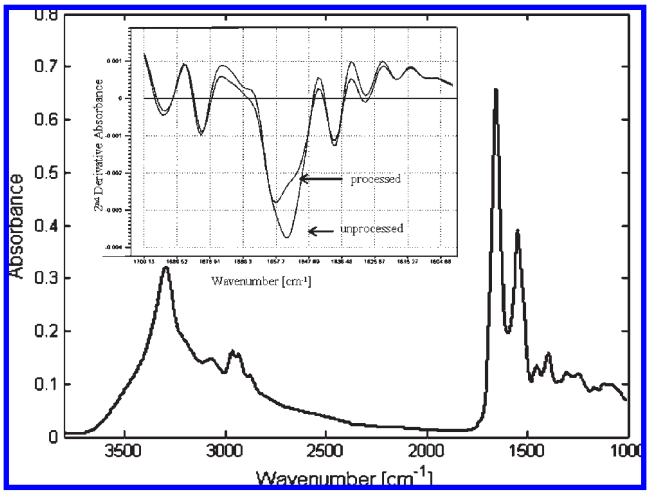

Figure 2. Typical FT-IR spectrum of a single myofiber obtained from unprocessed salmon muscle cryosection showing the spectral range from 4000 to 1000 cm^{-1}. (Inset) Positive second-derivative spectra of the same unprocessed sample together with a processed sample in the amide I region.

bands (1694, 1682, 1667, 1658, 1653, 1639, 1628, 1619, and 1609 cm^{-1}). Our findings are in agreement with earlier studies on fish, pork, and beef tissues (*5*, *19*−*24*). The band assignments are listed in **Table 2**.

Spectral Differences within Unprocessed Samples. Principal component analysis (PCA) was performed to study the unprocessed samples in the amide I region (1700−1600 cm^{-1}). The score plot of the first and second principal component based on 36 myofiber spectra (inside/skin side, head/tail, 3 different sizes) did not reveal any systematic clustering of the samples according to individual or sample position (results not shown). Higher principal components were also examined, and no systematic variations could be found. From these results, it can be concluded that, for the unprocessed samples, myofiber FT-IR spectra from different individuals and different locations show no systematic variation with respect to local variation within each salmon fillet and individuals.

Multivariate Analysis of Myofiber Spectra from Processed Salmon, Nonsmoked, and Smoked Samples

Analysis of Amide I. PCA was used to investigate the nonaveraged spectra of (salted) nonsmoked and smoked samples in the amide I region (1700−1600 cm^{-1}) (shown in **Figure 3**). The explained variances for PC1 and PC2 are 46% and 34%, respectively. The first principal component showed a systematic variation with respect to depth (difference between inside and skin side), whereas the second

Table 2. IR Region, FT-IR Frequencies, and Approximate Descriptions of Vibrational Modes

region	frequency (cm^{-1})	tentative band assignment
amide I	1694	aggregated β-sheet structures (intramolecular)
	1682	antiparallel β-sheet structures (intramolecular)
	1667	non-hydrogenated C=O groups
	1658	loop structures
	1653	α-helical structures
	1639	antiparallel β-sheet structures/O−H bending of water
	1628	aggregated β-sheet structures (intramolecular)
	1619	aggregated β-sheet structures (intermolecular)
	1609	amino acid side chains (tentatively)
amide II	1584	α-helical structures
	1574	unspecified
	1567	residue and/or possibly aggregated β-sheet structures
	1555	unspecified
	1544	α-helical structures
	1534	denatured random structures
	1526	aggregated β-sheet structures (tentatively)
	1510	tyrosine (tentatively)

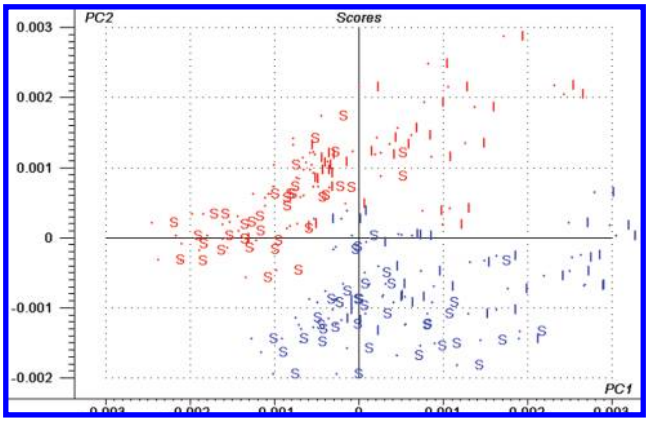

Figure 3. PCA score plot of nonaveraged samples (144 samples) using the selected wavenumbers of the inverted second derivative in the amide I region as variables. Marked in red: salted; in blue, smoked; S and I represent the skin side and inside samples, respectively. The explained variance by PC1 and PC2 is 46% and 34%, respectively.

principal component showed a systematic variation with respect to smoking. Inspecting the loading vector of component one, we found that the band near 1653 cm^{-1}, which is assigned to α-helical structures, contributed strongly (results not shown). It was shown that this band decreased in magnitude in inside samples of salmon fillets if we compare

with skin side samples, implying a loss of α-helical components. This may be explained by the fact that the skin of the fish protects the flesh near the skin from salt and smoke components. In addition, the fat deposited in the fish muscle acts as a barrier against the diffusion of these components from the inside to muscle regions near the skin during processing; consequently, the skin side locations are less accessible. In the following, we treat the spectra from inside and skin side locations separately.

PLSR was carried out to study the effect of the design factors on the FT-IR spectra of processed samples for skin side and inside samples separately. In the analysis, the **X** matrix contained the design parameters, while the **Y** matrix consisted of selected wavenumbers in the amide I region. In **Figure 4a** and **b**, the correlation loading plots of the first two PLS components of inside and skin side, respectively, are shown. The inner and outer circles in the figures refer to 50 and 100% explained variance, respectively. For the inside part samples (**Figure 4a**), the explained variance in **X** and **Y** for PLS components 1 and 2 are 23% and 23% for **X**, and 36% and 21% for **Y**. As **Figure 4a** shows, the salting time spans the first PLS component, while smoking spans the second PLS component. Samples salted for 24 h were highly correlated with bands 1628, 1694, 1682, and 1667 cm^{-1}, whereas samples salted for 8 h were well correlated with the band near 1653 cm^{-1}. This shows that longer salting periods resulting in higher salt concentrations (see **Table 1**) lead to a higher share of β-sheet structures and nonhydrogenated C═O groups, and a lower share of α-helical structure in the myofibers (see **Table 2**). These findings support the results obtained by previous studies related to different salt concentrations (*20*, *34*). Bocker and co-workers (*20*) showed that in pork muscle tissue subjected to brine salting at different salt concentrations (0.9, 3, 6, and 9% NaCl) the amount of α-helical structures (1653 cm^{-1}) was higher in samples with low salt content and that the level of nonhydrogenated C═O groups (1668 cm^{-1}) was increased at higher salt concentrations. Also another study (*22*) in pork tissue subjected to salting at different concentrations (3, 6, and 9% NaCl) revealed that salting induced an increase in aggregated β-sheet structure and a decrease in α-helical structure. A recent study by Bocker and co-workers (*5*) on brine salting (16% NaCl) of Atlantic salmon showed that the salt uptake varied due to the salmon raw material quality. The qualities that had higher salt content in the muscle presented an increase in the share of the 1668 cm^{-1} band.

Smoked and nonsmoked samples were separated along PLS 2. For nonsmoked samples, the absorbances at the bands near 1639 cm^{-1} and 1609 cm^{-1} were increased. The band at 1639 cm^{-1} was assigned both to antiparallel β-sheet structures (intramolecular) (*18*) and to O−H bending of water (*35*). Since smoked samples show a higher weight loss than nonsmoked ones (see **Table 1**), the decrease of absorption at 1639 cm^{-1} for the smoked sample may be explained by dehydration. Dehydration after smoking has been reported by several authors (*11*, *12*). The band at 1609 cm^{-1} has frequently been discussed to be related to amino acid side chains (*36*). In previous studies on muscle fiber tissues, this band has been tentatively assigned to the amino acid tyrosine (*23*, *24*). Since carbonyl compounds of smoke can react with amino groups of the protein chain and/or of the side chains as in a Maillard reaction, we may expect that in the present study the band at 1609 cm^{-1} is decreased in smoked samples, which is confirmed by **Figure 4a**.

For the skin side part samples (**Figure 4b**) the explained variance in **X** and **Y** for PLS components 1 and 2 was 22%

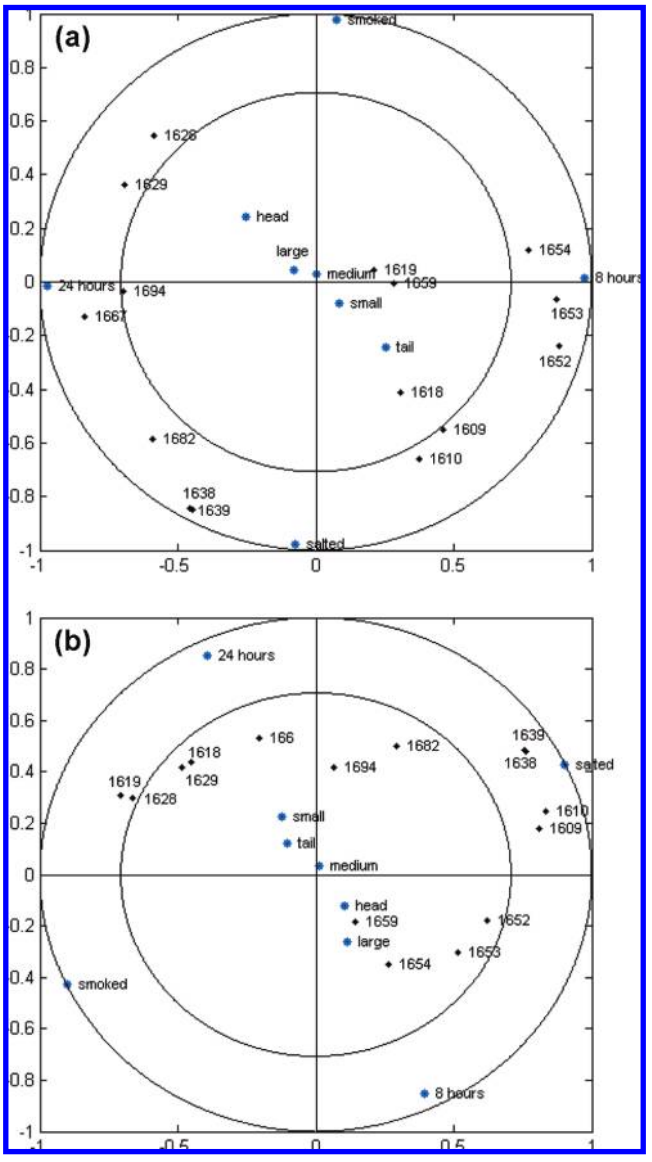

Figure 4. Correlation loading plots of PLSR with design parameters as X and selected wavenumbers of the inverted second derivative in the amide I region as Y. The inner and outer circles in the figure refer to 50 and 100% explained variance, respectively. For the inside part samples (**a**), the explained variance in **X** and **Y** for PLS components 1 and 2 are 23%, 23% for **X** and 36% and 21% for **Y**. For the skin side part samples (**b**), the explained variance in **X** and **Y** for PLS components 1 and 2 are 22% and 22% for **X** and 32% and 14% for **Y**.

and 22% for **X**, and 32% and 14% for **Y**, respectively. In contrast to the inside samples, for the skin side samples PLS1 is mainly explained by the smoking and to a lower degree by the salting time. This means that smoking introduces larger variations in the amide I region than salting time. Apart from this, the general picture in **Figure 4b** is unchanged and confirms the findings from **Figure 4a**.

Analysis of Amide II. In the second derivative spectra of the amide II region (1600−1500 cm^{-1}), the following bands were identified: 1584, 1574, 1567, 1555, 1544, 1534, 1526, and 1510 cm^{-1}. The band assignments are listed in **Table 2** together with the bands found in the amide I region. These bands were assigned and discussed previously for pork muscle fiber tissue (*21*).

PLSR was performed to study the effect of the design factors on the FT-IR spectra of processed samples in the

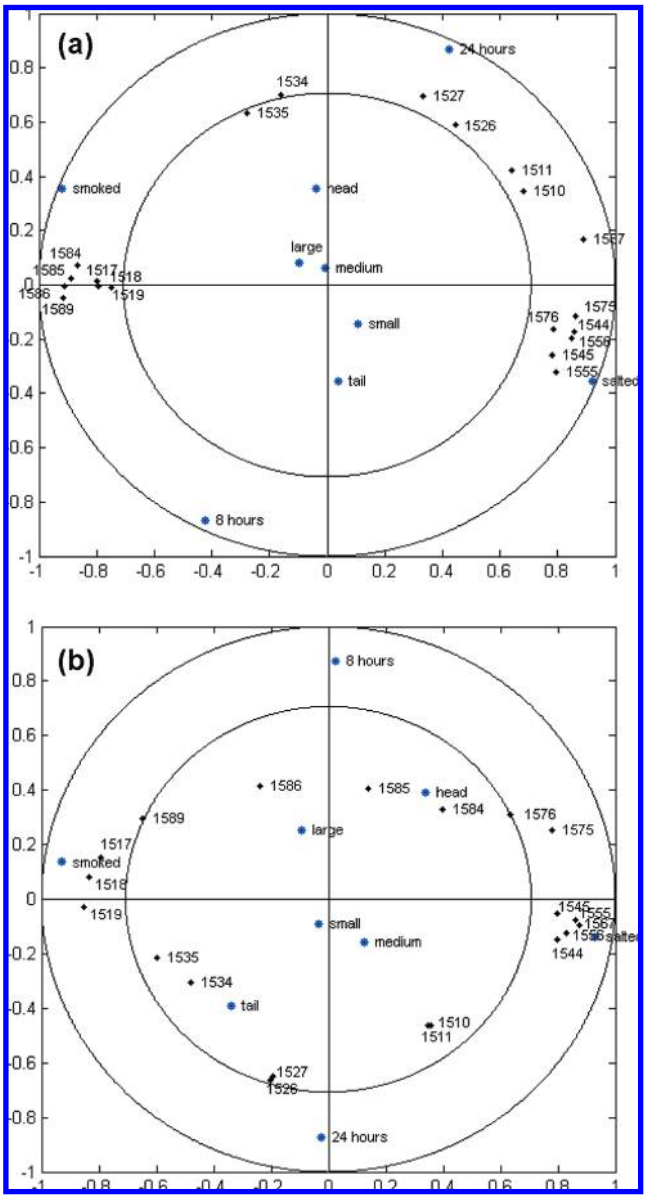

Figure 5. Correlation loading plots of PLSR with design parameters as X and selected wavenumbers in the amide II region of the negative 2nd derivative spectra as Y. The inner and outer circles in the figure refer to 50 and 100% explained variance, respectively. For the inside part (**a**), the first PLS component has an explained variance of 23% and 56% for **X** and **Y**, respectively, whereas the second PLS component has an explained variance of 23% and 12% in **X** and **Y**, respectively. For the skin side part (**b**), the first PLS component has an explained variance of 22% and 41% for **X** and **Y**, respectively, whereas the second PLS component has an explained variance of 22% and 11% in **X** and **Y**, respectively.

amide II region for the inside and skin side parts separately. The respective correlation loading plots are shown in **Figure 5a** and **b**. For the inside part (**Figure 5a**), the first PLS component has an explained variance of 23% and 56% for **X** and **Y**, respectively, whereas the second PLS component has an explained variance of 23% and 12% in **X** and **Y**, respectively. For the skin side part (**Figure 5b**), the first PLS component has an explained variance of 22% and 41% for **X** and **Y**, respectively, whereas the second PLS component has an explained variance of 22% and 11% in **X** and **Y**, respectively. An interesting result is that the main variation in the amide II region is due to smoking for both parts of the fillet (inside and skin side). Along PLS1, the smoked samples are totally separated from nonsmoked samples, whereas PLS2 separated the samples with regard to salting time.

The amide II region is well known to be conformationally sensitive, although it is more difficult to interpret than the amide I region. It is dominated by N−H bending (60%) and C−N stretching (40%) vibrations. In addition, it has been suggested that the contribution of amino acid side chains to the amide II region may be larger than that in the amide I region (*37*−*39*). As has been demonstrated in previous studies, the smoking process in some fish showed a decrease in the availability of lysine (*15*, *16*). Riha and co-workers (*15*) revealed that carbonyl compounds of liquid smoke solutions undergo a condensation reaction with amino groups of proteins where lysine appeared to be the most reactive amino acid. Moreover, Sisko and co-workers (*16*) also reported a lysine loss in smoked trout compared that in to nonsmoked trout. We may conclude that changes in the amide II region could be related to interactions between smoke components and amino groups from lysine or other N terminal of side chains more than specific protein secondary structural changes. This is also confirmed by the fact that in this kind of reactions N−H groups of proteins are interacting, which contribute strongly to the amide II region.

Comparison of Light Microscopy and FT-IR Microspectroscopy. Both FT-IR spectra and light microscopy images from salmon muscle tissue were compared after introducing variation due to salting and smoking. A longer salting period resulted in increased amounts of aggregated β-structures and in decreased amounts of α-helical structures as identified in the amide I region. These changes were related to observations made by light microscopy where salted samples appeared to be more detached and their extracellular spaces increased. However, smoking did not affect the same IR bands as salting. As was observed in amide I, the bands near 1639 cm^{-1} and 1609 cm^{-1} were decreased as a result of dehydration and interactions between smoke components and amino acid side chains. Moreover, in the amide II region, the major differences were caused by smoking. It is likely that the interaction between the carbonyl compounds of smoke and amino groups from lysine or other N terminal of side chains is the main contributor to the FT-IR signal in the amide II region. After smoking, light images showed that the myofibers of the smoked samples appeared to be more shrunken and that their shape appeared more irregular and edged than for the nonsmoked samples.

In conclusion, an understanding of the structural and chemical changes of food muscle proteins in smoking processes is crucial for the production of high quality smoked products. Most of the major quality issues in smoked salmon, such as water holding capacity and texture, are related to myofibrillar proteins. In the present study, it has been demonstrated for the first time that FT-IR microspectroscopy can be used to identify the interactions between proteins and smoke components. Furthermore, it has been shown that salting time is an important parameter in the cold smoking process, affecting the secondary structure of fish proteins. Data from this study can provide insights into the possibilities of FT-IR microspectroscopy as a nondestructive technique to monitor processing-induced changes in muscle tissues.

ACKNOWLEDGMENT

I.C. thanks Karin Solgaard, Frank Lundby, and Tom C. Johannenssen for technical assistance.

This study was supported by TRUEFOOD (Traditional United Europe Food), an Integrated Project financed by the European Commission under the Sixth Framework Programme (Contract no FOOD-CT-2006-016264). In addition, funding by the Ministerio de Educación y Ciencia (MEC, AGL-2006-01381) is gratefully acknowledged. I.C. thanks the Ministerio de Educación y Ciencia for a Predoctoral Fellowship.

LITERATURE CITED

(1) Birkeland, S.; Rora, A. M. B.; Skara, T.; Bjerkeng, B. Effects of cold smoking procedures and raw material characteristics on product yield and quality parameters of cold smoked Atlantic salmon (*Salmo salar* L.) fillets. *Food Res. Int*. **2004**, *37* 273–286.

(2) Official Codex Standards. Recommended International Code of Practice for Smoked Fish. CAC/RCP 25-1979, 9, 1−44.

(3) Hamm, R. Functional Properties of the Myofibrillar System and Their Measurements. In *Muscle As Food*; Bechtel, P. J., Ed.; Academic Press: New York 1986; pp 135−199.

(4) Barat, J. M.; Rodriguez-Barona, S.; Andres, A.; Fito, P. Influence of increasing brine concentration in the cod-salting process. *J. Food Sci*. **2002**, *67*, 1922–1925.

(5) Bocker, U.; Kohler, A.; Aursand, I. G.; Ofstad, R. Effects of brine salting with regard to raw material variation of Atlantic salmon (*Salmon salar*) muscle investigated by FT-IR microspectroscopy. *J. Agric. Food Chem*. **2008**, *56*, 5129–5137.

(6) Suñen, E.; Fernandez-Galian, B.; Aristimuno, C. Antibacterial activity of smoke wood condensates against *Aeromonas hydrophila*, *Yersinia enterocolitica* and *Listeria monocytogenes* at low temperature. *Food Microbiol*. **2001**, *18*, 387–393.

(7) Guillen, M. D.; Cabo, N. Study of the effects of smoke flavorings on the oxidative stability of the lipids of pork adipose tissue by means of Fourier transform infrared spectroscopy. *Meat Sci*. **2003**, *66*, 647–657.

(8) Leroi, F.; Joffraud, J. J. Salt and smoke simultaneously affect chemical and sensory quality of cold-smoked salmon during 5 °C storage predicted using factorial design. *J. Food Prot*. **2000**, *63*, 1222–1227.

(9) Rorvik, L. M. *Listeria monocytogenes* in the smoked salmon industry. *Int. J. Food Microbiol*. **2000**, *62*, 183–190.

(10) Sigurgisladottir, S.; Sigurdardottir, M. S.; Ingvarsdottir, H.; Torrissen, O. J.; Hafsteinsson, H. Microstructure and texture of fresh and smoked Atlantic salmon, *Salmo salar* L., fillets from fish reared and slaughtered under different conditions. *Aquac. Res*. **2001**, *32*, 1–10.

(11) Hultmann, L.; Bencze Rora, A. M.; Steinsland, I.; Skara, T.; Rustad, T. Proteolytic activity and properties of proteins in smoked salmon (*Salmo salar*) effects of smoking temperature. *Food Chem*. **2003**, *85*, 377–387.

(12) Gomez-Guillen, M. C.; Montero, P.; Hurtado, O.; Borderias, A. J. Biological characteristics affect the quality of farmed Atlantic salmon and smoked muscle. *J. Food Sci*. **2000**, *65* 53–60.

(13) Dvorak, Z.; Vognarova, I. Available lysine in meat and meat products. *J. Sci. Food Agric*. **1965**, *16*, 305–312.

(14) Chen, L.-B.; Issenberg, P. Interactions of some wood smoke components with e-amino groups in proteins. *J. Agric. Food Chem*. **1972**, *20*, 1113–1115.

(15) Riha, W. E.; Wendorff, W. L. Browning potential of liquid smoke solutions: comparison of two methods. *J. Food Sci*. **1993**, *58*, 671–674.

(16) Siskos, I.; Zotos, A.; Taylor, K. D. A. The effect of drying, pressure and processing time on the quality of liquid-smoked trout (*Salmo gairdnerii*) fillets. *J. Sci. Food Agric*. **2005**, *85*, 2054–2060.

(17) Metz, B.; Kersten, G. F. A.; Hoogerhout, P.; Brugghe, H. F.; Timmermans, H.A M; de Jong, A.; Meiring, H.; Ten, H. J.; Hennink, W. E.; Crommelin, D. J. A.; Jiskoot, W. Identification of formaldehyde-induced modifications in proteins: reactions with model peptides. *J. Biol. Chem*. **2004**, *279* 6235–6243.

(18) Jackson, M.; Mantsch, H. H. The use and misuse of FT-IR spectroscopy in the determination of protein structure. *Crit. Rev. Biochem. Mol. Biol*. **1995**, *30*, 95–120.

(19) Kirschner, C.; Ofstad, R.; Skarpeid, H. J.; Host, V.; Kohler, A. Monitoring of denaturation processes in aged beef loin by Fourier transform infrared microspectroscopy. *J. Agric. Food Chem*. **2004**, *52*, 3920–3929.

(20) Bocker, U.; Ofstad, R.; Bertram, H. C.; Egelandsdal, B.; Kohler, A. Salt-induced changes in pork myofibrillar tissue investigated by FT-IR microspectroscopy and light microscopy. *J. Agric. Food Chem*. **2006**, *54*, 6733–6740.

(21) Bocker, U.; Ofstad, R.; Wu, Z.; Bertram, H. C.; Sockalingum, G. D.; Manfait, M.; Egelandsdal, B.; Kohler, A. Revealing covariance structures in Fourier transform infrared and Raman microspectroscopy spectra: a study on pork muscle fiber tissue subjected to different processing parameters. *Appl. Spectrosc*. **2007**, *61*, 1032–1039.

(22) Wu, Z.; Bertram, H. C.; Kohler, A.; Bocker, U.; Ofstad, R.; Andersen, H. J. Influence of Aging and salting on protein secondary structures and water distribution in uncooked and cooked pork. A combined FT-IR microspectroscopy and ^{1}H NMR relaxometry study. *J. Agric. Food Chem*. **2006**, *54* 8589–8597.

(23) Wu, Z.; Bertram, H. C.; Bocker, U.; Ofstad, R.; Kohler, A. Myowater dynamics and protein secondary structural changes as affected by heating rate in three pork qualities: a combined FT-IR microspectroscopic and ^{1}H NMR relaxometry study. *J. Agric. Food Chem*. **2007**, *55*, 3990–3997.

(24) Bertram, H. C.; Kohler, A.; Bocker, U.; Ofstad, R.; Andersen, H. J. Heat-induced changes in myofibrillar protein structures and myowater of two pork qualities. A combined FT-IR spectroscopy and low-field NMR relaxometry study. *J. Agric. Food Chem*. **2006**, *54*, 1740–1746.

(25) Engdahl, A.; Kolar, K. Metodeforskrift 22.6.93 Koksaltbestamning med Corning 926 Chloride Analyzer, Kottforskningsinstitut I Kavlinge, 1993.

(26) Savitzky, A.; Golay, M. J. E. Smoothing and differentiation of data by simplified least squares procedures. *Anal. Chem*. **1964**, *36*, 1627–1639.

(27) Kohler, A.; Kirschner, C.; Oust, A.; Martens, H. Extended multiplicative signal correction as a tool for separation and characterization of physical and chemical information in Fourier transform infrared microscopy images of cryo-sections of beef loin. *Appl. Spectrosc*. **2005**, *59* 707–716.

(28) Martens, H.; Martens, M., *Multivariate Analysis of Quality: An Introduction*; John Wiley & Sons Ltd.: Chichester, UK, 2001.

(29) Aursand, I. G.; Veliyulin, E.; Bocker, U; Ofstad, R.; Rustad, T.; Erikson, U. Water and salt distribution in Atlantic salmon (*Salmo salar*) studied by low-field ^{1}H-NMR, ^{1}H and ^{23}Na MRI and light microscopy: Effects of raw material quality and brine salting. *J. Agric Food.Chem*. **2009**, *57*, 46–54.

(30) Wang, D.; Tang, J.; Correia, L. R. Salt diffusivities and salt diffusion in farmed Atlantic salmon muscle as influenced by rigor mortis. *J. Food Eng*. **2000**, *43*, 115–123.

(31) Segtnan, V. H.; Høy, M.; Sørheim, O.; Kohler, A.; Lundby, F.; Wold, J. P.; Ofstad, R. Noncontact salt and fat distributional analysis in salted and smoked salmon fillets using X-ray computed tomography and NIR interactance imaging. *J. Agric. Food Chem*. **2009**, *57*, 1705–1710.

(32) Cardinal, M.; Knockaert, C.; Torrissen, O.; Sigurgisladottir, S.; Morkore, T.; Thomassen, M.; Vallet, J. L. Relation of smoking parameters to the yield, color and sensory quality of smoked Atlantic salmon (*Salmo salar*). *Food Res. Int*. **2001**, *34*, 537–550.

(33) Krimm, S.; Bandekar, J. Vibrational spectroscopy and conformation of peptides, polypeptides, and proteins. *Adv. Protein Chem*. **1986**, *38*, 181–364.

(34) Stafford, W. F. Effect of various anions on the stability of the coiled coil of skeletal muscle myosin. *Biochemistry* **1985**, *24*, 3314–3321.
(35) Jackson, M.; Choo, L. P.; Watson, P. H.; Halliday, W. C.; Mantsch, H. H. Beware of connective-tissue proteins: Assignment and implications of collagen absorptions in infrared-spectra of human tissues. *Biochim. Biophys. Acta* **1995**, *1270*, 1–6.
(36) Fabian, H; Mantele, W. Infrared Spectroscopy of Proteins. In *Handbook of Vibrational Spectroscopy*; Chalmers, J. M., Griffiths, P. R., Eds.; John Wiley & Sons Ltd.: Chichester, U.K., 2002; pp 3399−3425.
(37) Chirgadze, Y. N.; Fedorov, O. V.; Trushina, N. P. Estimation of amino acid residue side-chain absorption in the infrared spectra of protein solutions in heavy water. *Biopolymers* **1975**, *14*, 679–694.
(38) Venyaminov, S. Y.; Kalnin, N. N. Quantitative IR spectrophotometry of peptide compounds in water (H_2O) solutions. I. Spectral parameters of amino acid residue absorption bands. *Biopolymers* **1990**, *30*, 1243–1257.
(39) Fabian, H.; Naumann, D. Methods to study protein folding by stopped-flow FT-IR. *Methods* **2004**, *34*, 28–40.

Received for Review November 25, 2008. Accepted February 25, 2009. Revised manuscript received February 18, 2009. The information in this document reflects only the authors' views, and the Community is not liable for any use that may be made of the information contained therein.